International Journal of Applied Engineering Research
ISSN 0973-4562 Volume 10, Number 7 (2015) pp. 17085-17101

http://www.ripublication.com

Comparison of Different Control Techniques For DSTATCOM With PV Array For Power Quality Improvement

M.Manoj Kumar[1], J.Jayachandran [2], S.Malathi [3]
[1]PG-Scholar, [2]Senior Assistant Professor, [3]Assistant Professor
School of Electrical and Electronics Engineering, SASTRA University,
Thanjavur – 613401, Tamilnadu, India
Email id: manepallimanojkumar@gmail.com

Abstract

In this paper, the assessment of different control techniques used in Distributed Static Compensator (DSTATCOM) is analysed. The control techniques which are compared in this paper are Synchronous Reference Frame (SRF) theory, Adaptive Filter based on synchronous extraction, Modified SRF theory. A Photo Voltaic (PV) array is modelled and proposed for feeding the three phase Voltage Source Inverter (VSI) incorporated with a boost converter to enhance the PV array voltage to meet the DC bus voltage. The above stated control strategies are implemented to generate the firing pulses to the VSI which will improve the power quality of the system. These models are fabricated and developed in MATLAB/SIMULINK environment with non-linear and unbalanced load conditions. In all the control strategies, the source current %THD is brought down below 5% which meets out the IEEE-519 standards.

Keywords: DSTATCOM, Power quality improvement, Total Harmonic Distortion (THD), Solar panel, boost converter, PI controller, Reactive power

Introduction

In recent era, the power quality improvement using renewable resources has been concentrated by many scholars owing to the proliferation of the non-linear loads in the distribution side [1]. Maximum of the electrical loads utilized now-a-days are having non-linear characteristics. e.g. SMPS, motor drive applications, computer loads, ballasts etc. These loads are the main reason for the generation of harmonics in supply current which also exceeds the neutral current. There are various renewable sources like PV, wind power, fuel cell, tidal power, geothermal, etc. In this paper, PV array is used for power quality improvement. The PV cell is having the proficiency to

connect in series and parallel for increasing the voltage and current magnitudes correspondingly. The power produced from the solar panel require power conditioning before linking it to the dc bus capacitor and the voltage level is also not adequate to meet the reference value. So, it is prerequisite to connect a boost converter for increasing the voltage magnitude. The stepped up voltage from boost converter is fed to the dc bus thereby the voltage is maintained constant.

The distribution system is under extreme power quality problems because of the non-linear loads. Harmonic currents, load unbalance, high reactive power demand and extravagant neutral currents are the problems faced in the distribution side. So Custom Power Devices (CPDs) like DSTATCOM, Dynamic Voltage Restorer (DVR), and Unified Power Quality Conditioner (UPQC) are applied to provide solutions to the above stated issues. DSTATCOM is used in this paper to mitigate the above power quality issues. A comparison is performed with three different control strategies for same load and source conditions. The control strategies used in this paper are SRF theory, Adaptive filter based on synchronous extraction and a modified SRF theory.

System Configuration of DSTATCOM

A solar array is connected as the input to the boost converter whose output is fed as input to the DC link capacitor (C_{dc}). This DC link capacitor acts as the source to the Voltage source inverter (VSI). The switching devices which are used in VSI are Insulated Gate Bipolar Transistor (IGBT's). An inductor is used at the output of the VSI which is used to filter out the ripple content in the output current. A ripple filter which is connected at the Point of Common Coupling (PCC) is to minimise the ripple voltage owing to the switching current at the VSI. Fig.1. depicts the block diagram of the proposed model.

The value of voltage which is to be maintained across the DC link is calculated with respect to the output voltage of VSI. The expression for voltage across DC link is given by eqn.(1)

$$V_{dc} = \frac{2\sqrt{2}V_{L-L}}{\sqrt{3}m} \tag{1}$$

Where $V_{L\text{-}L}$ is the line to line voltage which is taken as 415V and m signifies the modulation index which is considered as 1. By calculating V_{dc}, we get the value as 677.6V and it is rounded off to 678V.

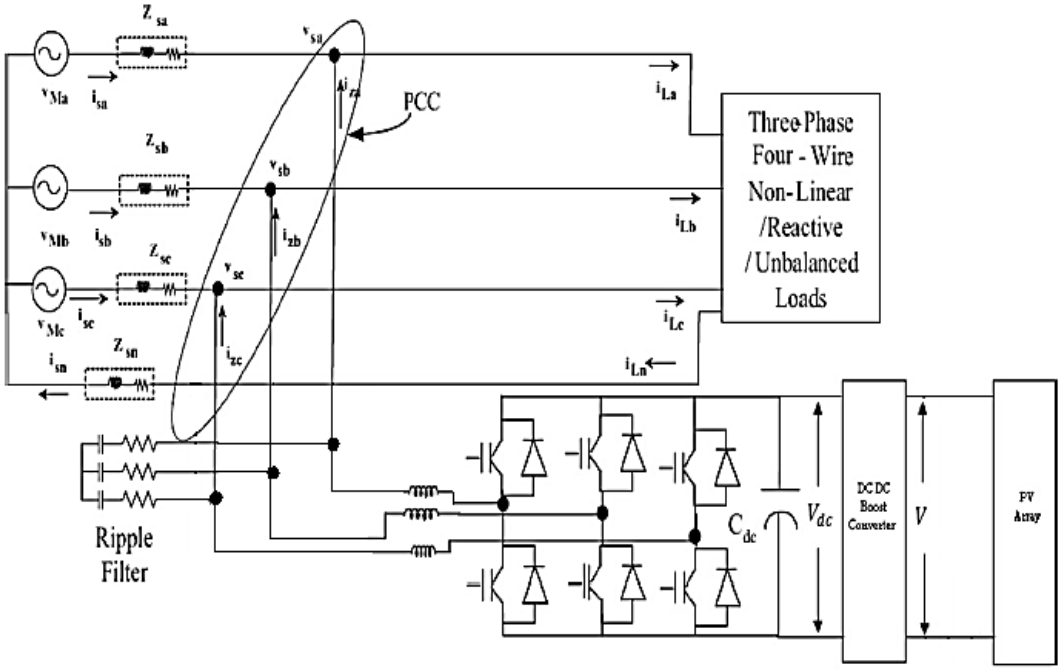

Figure 1: System Configuration of Proposed System

Modelling of PV Array

A PV array comprises of several PV cells which are connected in series and parallel. These PV cells are having the proficiency to connect in series and parallel for increasing the voltage and current magnitudes respectively [3]-[5]. Fig.2 depicts the electrical equivalent of Solar cell.

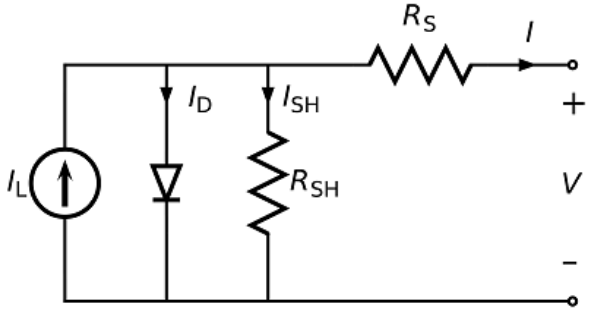

Figure 2: Electrical Equivalent of A Solar Cell

The model of PV panel is prepared in MATLAB using the parameters which are available from SANYO-240HDE4 datasheet at an irradiation 1000W/m^2 and at 25^{o}C temperature. The specifications of the solar panel is shown in Table.1

Table 1: Specifications of the Solar Panel Used

Parameters	**Symbol**	**Typical value**
Rated maximum power	P_{mp}	240W
Open circuit voltage	V_{oc}	43.6
Short circuit current	I_{sc}	7.37
Rated voltage	V	35.5
Rated current	I	6.77
Short circuit temperature coefficient	K_i	2.21mA/oC
Open circuit temperature coefficient	Kv	1.0109V/oV
Number of cells	-	10x6

For modelling a Solar cell, equation (2) is taken into consideration. The equation for the cell current (I_m) is

$$I_m = I_{pv} - I_o\left(e^{\frac{V+IR_s}{V_T}} - 1\right) - \frac{V + IR_s}{R_p} \tag{2}$$

Where I_{pv} is the photo current, I_o is the diode reverse saturation current given by $I_o = \frac{I_{pv}}{e^{(V_{oc}/V_T)} - 1}$, V is the cell voltage, R_s denotes series resistance, R_p denotes shunt resistance, V_T denotes thermal voltage which is equal to $V_T = \frac{kT}{q}$ (Where k is Boltzmann constant and q is the charge of electron). The photo current is given by eqn.(3)

$$I_{pv} = (I_{scr} + k_i(\Delta T))\frac{G}{10} \tag{3}$$

Where I_{scr} is short circuit current at reference temperature, ΔT is change in temperature in Kelvin and G is Irradiance in W/m^2

The V-I characteristics of the above mentioned solar panel are shown in figure (3).

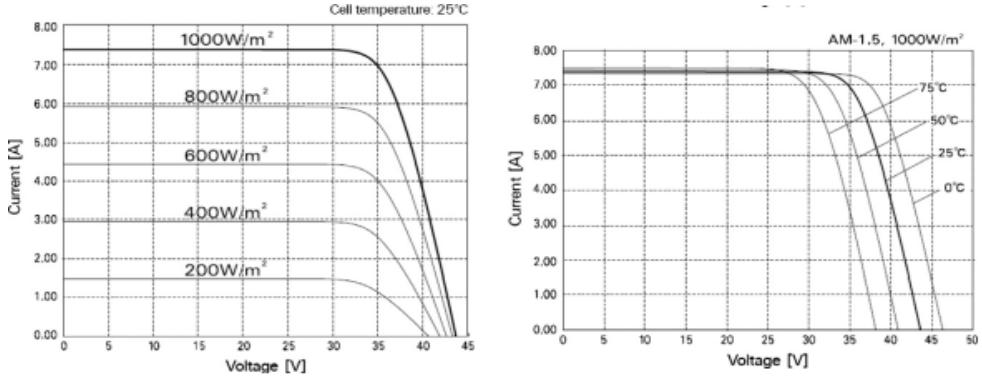

Figure 3: V-I Characteristics of Solar Panel

Control of Dc Bus Voltage Using Boost Converter

A boost converter will enhance the input voltage to the required output voltage. Boost converter is fed from the PV array. The basic working principle of a boost converter can be illustrated in two modes. In Mode 1, when the switch (SW) is turned ON, inductor stores energy from the input. In Mode2, when the switch (SW) is turned OFF, the source voltage is added up with the inductor voltage and the current is flown via diode to the load. Hence the voltage is boosted up [6]. The boost converter circuit diagram is depicted in the Fig.4.

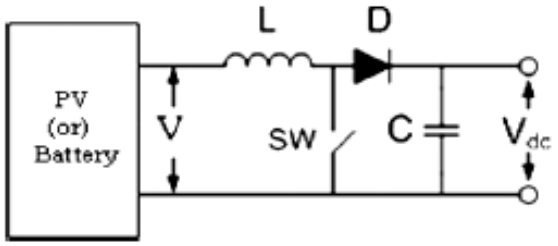

Figure 4: PV Panel and Boost Converter

By choosing an appropriate duty cycle, the boost converter output voltage is maintained at 676V. The expression for boosted output voltage is given by $\frac{V_{out}}{V_{in}} = \frac{1}{1-D}$ and $D = \frac{T_{ON}}{T_{ON} + T_{OFF}}$ where D denotes duty cycle, T_{ON} and T_{OFF} are the ON and OFF time periods respectively.

Control of DSTATCOM

In this paper the performance of three control schemes are analysed using MATLAB/Simulink software. They are SRF theory, Adaptive Filter based on synchronous extraction and a modified SRF theory.

A. Synchronous Reference Frame (SRF) theory

The block diagram of SRF controller is depicted in Fig.5. Feedback signals are sensed from several points like DC link voltage of STATCOM, PCC voltages, load currents and source currents [1]. The load currents are transformed from abc frame to dq0 frame using the equation (4).

$$\begin{bmatrix} i_d \\ i_q \\ i_o \end{bmatrix} = \frac{2}{3}\begin{bmatrix} \cos\theta & -\sin\theta & \frac{1}{2} \\ \cos(\theta-\frac{2\pi}{3}) & -\sin(\theta-\frac{2\pi}{3}) & \frac{1}{2} \\ \cos(\theta+\frac{2\pi}{3}) & \sin(\theta-\frac{2\pi}{3}) & \frac{1}{2} \end{bmatrix}\begin{bmatrix} i_{la} \\ i_{lb} \\ i_{lc} \end{bmatrix} \tag{4}$$

Where i_{la}, i_{lb} and i_{lc} are the load currents which are sensed. A Phase Locked Loop (PLL) is employed to synchronisation purpose. The transformed dq0 components are fed to a Low pass filter in order to acquire the DC components. Two inputs are fed into the PI controller 1 i.e. V_{dc} and V_{dc}^*. The two inputs are compared and then the error is fed into PI controller 1. The signal from the PI controller 1 is loss component of current (I_{loss}) as mentioned in the eqn. (5).

$$i_{loss(n)} = i_{loss(n-1)} + k_{pd}(V_{de(n)} - V_{de(n-1)}) + k_{id} v_{de(n)} \tag{5}$$

Where $V_{de(n)}$ is the error occurred at the n^{th} sampling instant of Reference DC bus voltage and the sensed DC bus voltage. k_{id} and k_{pd} denotes the integral and proportional gains of PI controller. The direct axis component of reference current (i_d^*) is given by eqn. (6)

$$i_d^* = i_{ddc} + i_{loss} \tag{6}$$

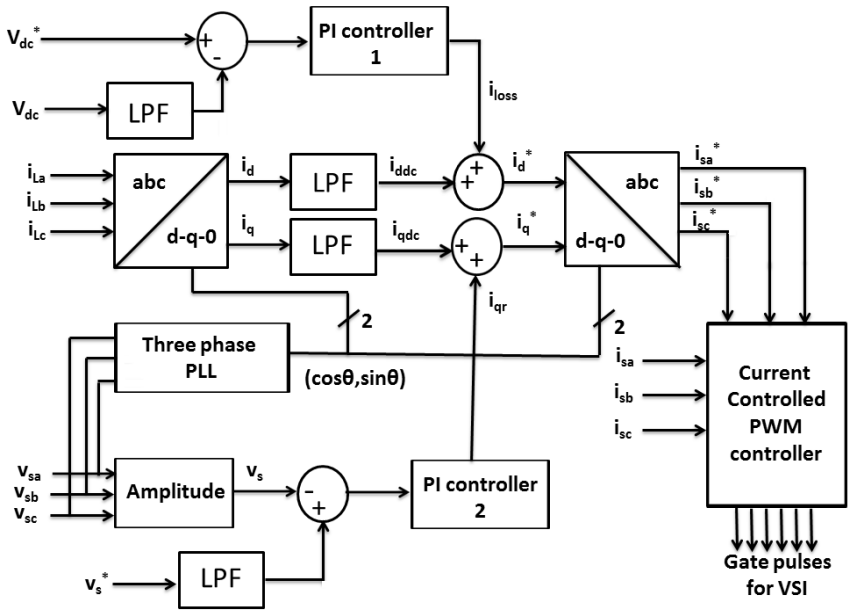

Figure 5: Controller For SRF Theory

Likewise the error between the amplitude and the reference value of PCC voltage is given to PI controller 2 and the output signal from the PI controller 2 is the quadrature current component (i_{qr}) derived using eqn. (7)

$$i_{qr(n)} = i_{qr(n-1)} + k_{pq}(V_{te(n)} - V_{te(n-1)}) + k_{iq} v_{te(n)} \quad (7)$$

Where $V_{te(n)}$ is the error value which is given to the PI controller at the n^{th} sampling time. k_{iq} and k_{pq} denotes the integral and proportional gains of PI controller. The reference value of quadrature current component (i_q^*) is expressed in the eqn. (8)

$$i_q^* = i_{qdc} + i_{qr} \quad (8)$$

B. Adaptive Filter (AF) based on synchronous extraction

In this control strategy, the reference currents are derived in the time domain using synchronous extraction [8]. The elementary steps involved in the control algorithm are

(i) Estimation of Cos and Sin Components of The PCC Voltages

$\sin\theta_{va}$ and $\cos\theta_{va}$ are the sine and cosine components of phase 'a' which are obtained using sinusoidal tracking algorithm. The block diagram of sinusoidal tracking algorithm is depicted in the figure 6.

A_1, A_2 and A_3 are the internal constants in the algorithm which are used to choose the accuracy and speed [7]. The outputs from this block are the in-phase and quadrature components of PCC voltage of phase 'a' v_{pa} and v_{qa}. PCC voltage amplitude is given by eqn. (9)

$$V_t = \sqrt{\frac{2}{3}(v_{sa}^2 + v_{sb}^2 + v_{sc}^2)} \quad (9)$$

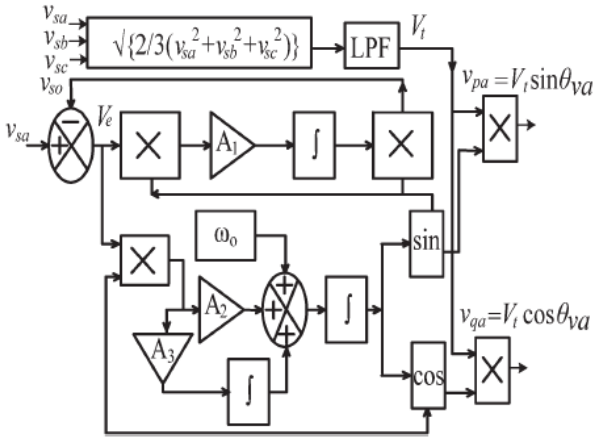

Figure 6: Sinusoidal Tracking Algorithm

Where v_{sa}, v_{sb} and v_{sc} are the PCC phase voltages. Similar estimation is done for other two phases 'b' and 'c'. The sine and cosine components derived for other two phases are $Sin\theta_{vb}$, $Sin\theta_{vc}$, $cos\theta_{vb}$ and $cos\theta_{vc}$.

(ii) Estimation of Load Current's Magnitude For Active and Reactive Component

By performing necessary mathematical calculations, the output derived is the active and reactive component I_{Lpa} and I_{Lqa} which are with respect to the phase 'a'. Similarly the estimation of other two phases is done [8]. The magnitude of real and reactive power components of 3-phase load currents are calculated using sum of individual magnitudes of real and reactive power current components which is divided by 3 . This is mathematically expressed in eqn. (10)

$$I_{LpA} = (i_{Lpa} + i_{Lpb} + i_{Lpc})/3$$
$$I_{LqA} = (i_{Lqa} + i_{Lqb} + i_{Lqc})/3 \quad (10)$$

(iii) Estimation of Reference Source Current's Magnitude For Real And Reactive Component

The input for PI controller 1 is the error amongst the sensed DC bus voltage (V_{dc}) and the reference DC bus voltage (V_{dc}*). The output of this PI controller is the current loss component (I_{loss}). The magnitude of active component of reference source current (I_{spt}) is the sum of loss current component I_{loss} and the average value of active load currents (I_{LpA}) is showm in eqn. (11).

i.e. $$I_{spt} = I_{loss} + I_{LpA} \quad (11)$$

Likewise the error between the amplitude and the reference value of PCC voltage is given as input to the PI controller 2 and the output signal is the quadrature current component (I_{qr}). The magnitude of reactive component of supply reference current (I_{sqt}) is the difference between I_{qr} and the average value of the reactive load current (I_{LqA}) which is depicted in eqn. (12.)

$$I_{sqt} = I_{qr} - I_{LpA} \quad (12)$$

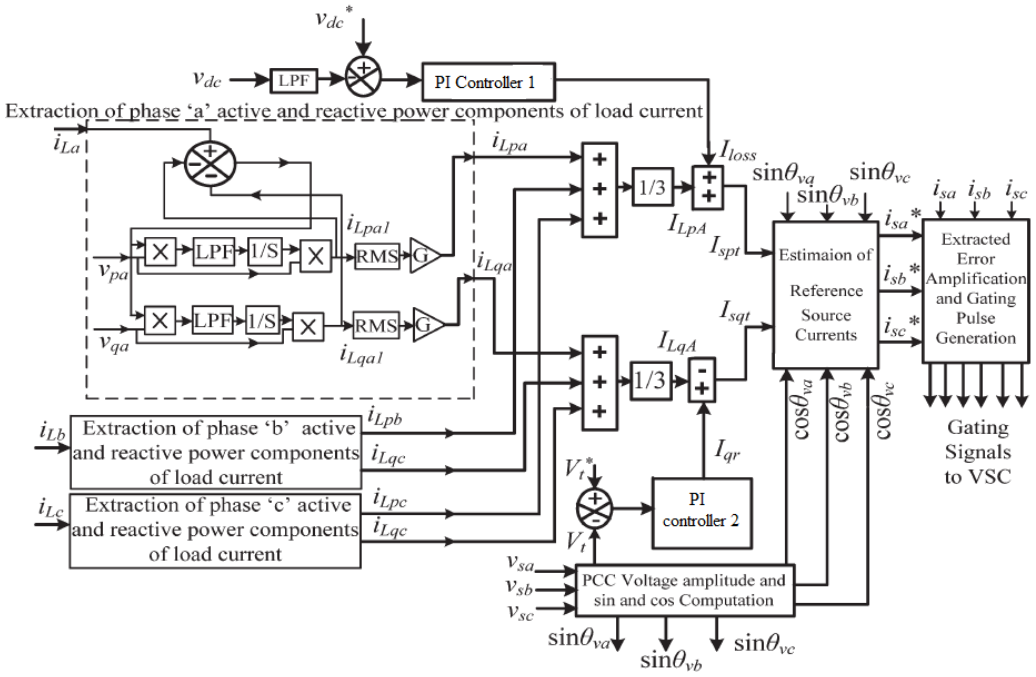

Fig.7 Adaptive filter controller

(iv) Estimation of Reference Source Current and PWM Pulse Generation

The real and reactive components of reference source currents are determined using the eqn. (13)

$$\begin{aligned} i_{sap} &= I_{spt}\sin\theta_{va} \qquad i_{saq} = I_{sqt}\cos\theta_{va} \\ i_{sbp} &= I_{spt}\sin\theta_{vb} \text{ and } i_{sbq} = I_{sqt}\cos\theta_{vb} \\ i_{scp} &= I_{spt}\sin\theta_{vc} \qquad i_{scq} = I_{sqt}\cos\theta_{vc} \end{aligned} \tag{13}$$

Therefore the reference source currents are derived from eqn. (14)

$$\begin{aligned} i_{sa}^* &= i_{sap} + i_{saq} \\ i_{sb}^* &= i_{sbp} + i_{sbq} \\ i_{sc}^* &= i_{scp} + i_{scq} \end{aligned} \tag{14}$$

The reference and sensed source currents are compared and the PWM pulses are generated which are given as the firing pulses to the VSI.

C. Modified SRF Theory

This modified SRF method is used to mitigate the harmonics with more precision in real time applications. The control algorithm of this Modified SRF theory is shown in the Fig.9. This method contains generation of unit vector, d-q transformation, harmonic current controller, regulation of DC link voltage and generating PWM pulses [11].

Generation of unit vector is performed in the easiest and efficient method as shown in the Fig.8. For the generation of unit vector, the instantaneous supply voltages are sensed. These supply voltages are transformed to 2-phase stationary $\alpha-\beta$ voltages using the Clarke's transformation and theses signals are fed to a 1st order low pass filter in order to get the DC components. This method of generation of unit vector leads to the exclusion of high frequency noises, grid harmonics and reactive power disturbances.

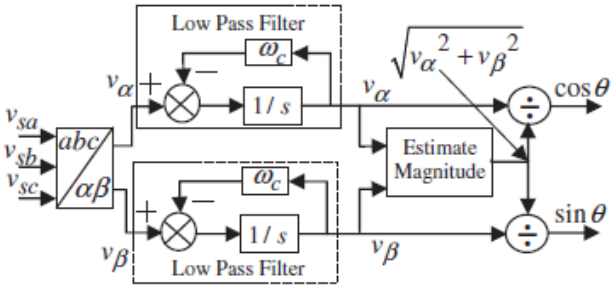

Figure 8: Generation of Unit Vector

These $\alpha-\beta$ components are transformed to the synchronous rotating reference frame d-q frame using the parks transformation. In the similar manner, the filter currents are also transformed from abc to d-q frame of reference.

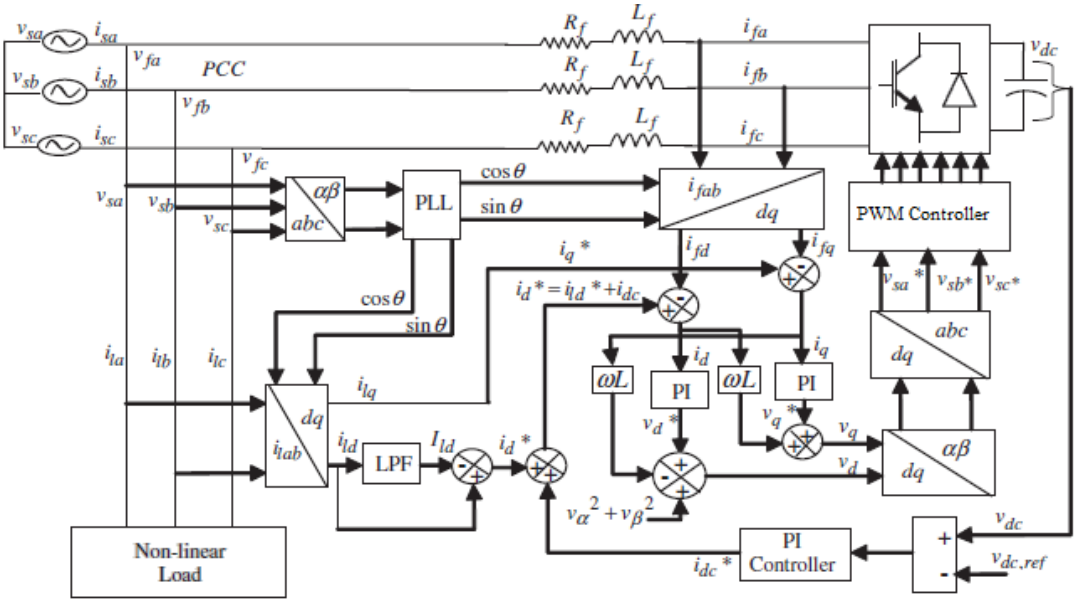

Figure 9: Modified SRF Controller

The inner current loop control is shown in the Fig.10. These are controlled using a PI controller. This can be achieved using the equation (15).

$$v_d^* = k_p i_d + k_i \int i_d dt$$
$$v_q^* = k_p i_q + k_i \int i_q dt \quad (15)$$

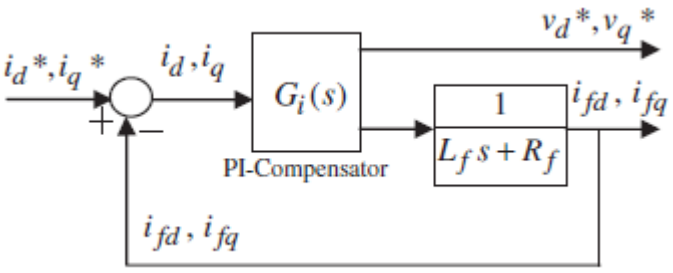

Figure 10: Inner Harmonic Current Loop Control

Where i_d and i_q are the current errors. The PI controller transfer function is given in eqn.16

$$G_i(s) = \frac{V_d(s)}{I_d(s)} = \frac{V_q(s)}{I_q(s)} = k_p \frac{s + k_i / k_p}{s} \quad (16)$$

The error amongst the DC bus voltage (V_{dc}) and the reference DC bus voltage (V_{dc}*) is given as input to a PI controller so that the voltage across the capacitor is maintained constant. A PWM generator is used to generate the pulses and these pulses are given to the VSI.

Results and Waveforms

A. SRF Theory

The waveforms of load and source currents using SRF theory are shown in Fig.11(a) and 11(b)

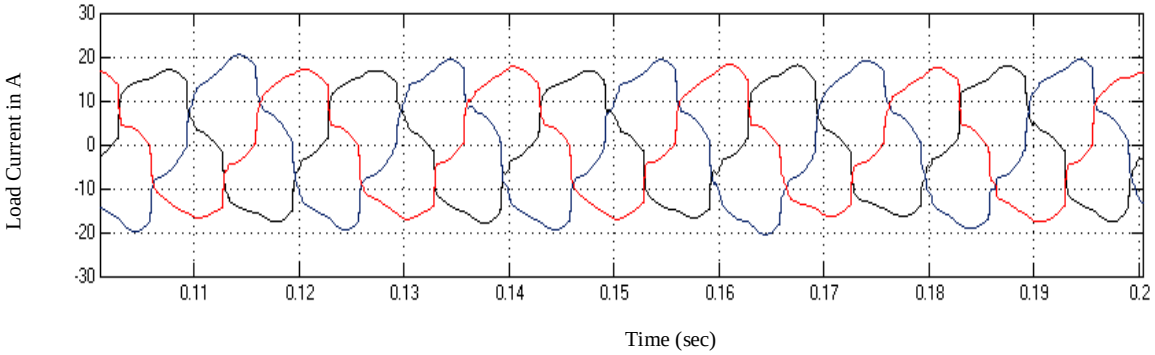

Figure 11(a): Load current waveform for SRF controller

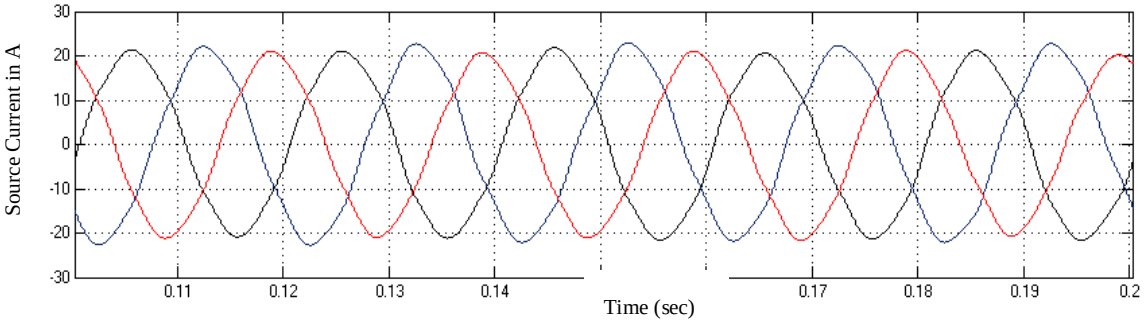

Figure 11(b): Source Current Waveform For SRF Controller

The THD analyses for load and source currents are shown in Fig. 11(c) and 11(d)

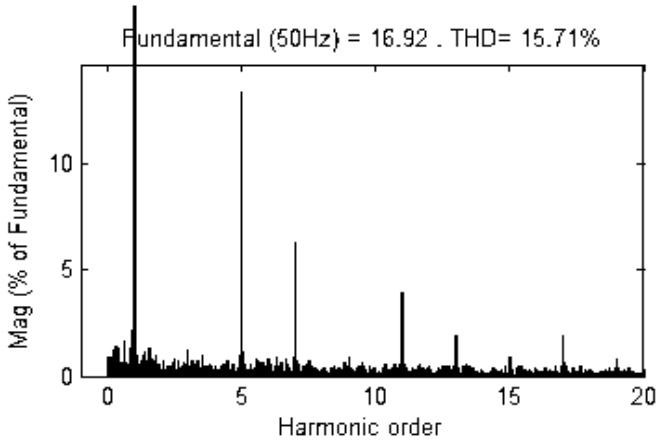

Figure 11(c): Load current THD

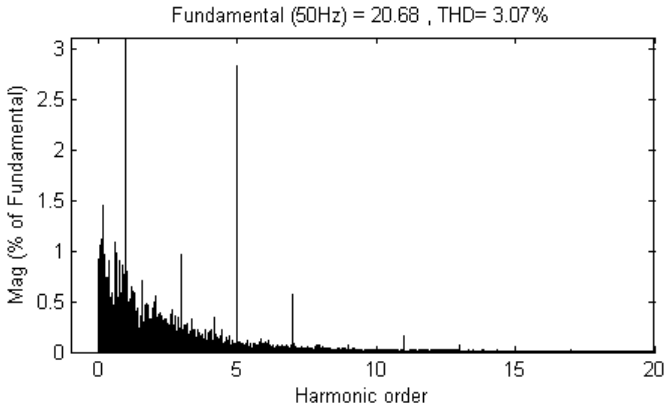

Figure 11(d): Source current THD

B. Adaptive filter control strategy

The waveforms of load and source currents using Adaptive Filter (AF) control strategy are depicted in Fig.12(a) and 12(b)

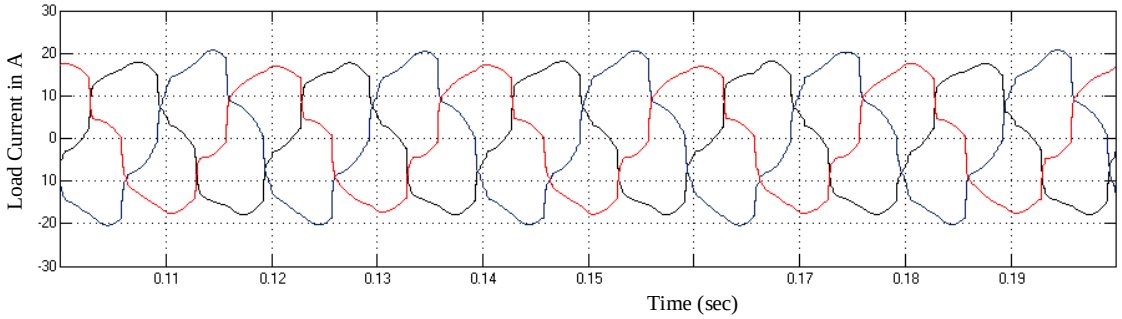

Figure 12(a): Load current waveform for Adaptive filter

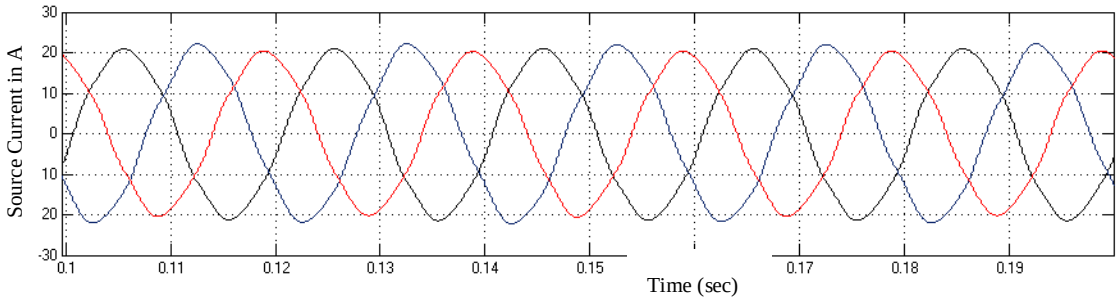

Figure 12(b): Source Current Waveform For Adaptive Filter

The THD analyses for load and source currents are depicted in Fig. 12(c) and 12(d)

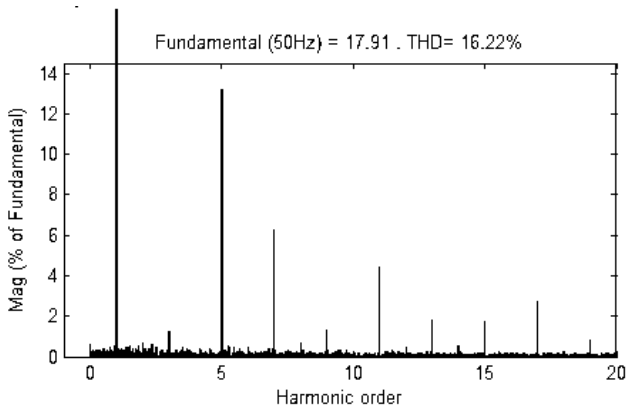

Figure 12(c): Load current THD

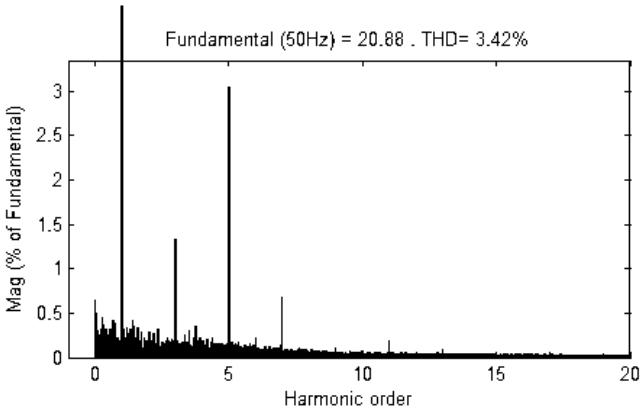

Figure 12(d): Source Current THD

C. Modified SRF Theory

The waveforms of load and source currents in Modified SRF theory are shown in Fig.13(a) and 13(b)

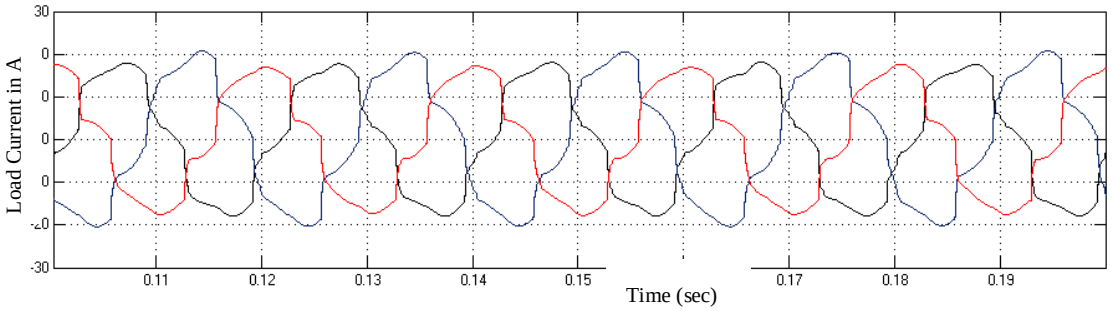

Figure 13(a): Load Current Waveform For Modified SRF Theory

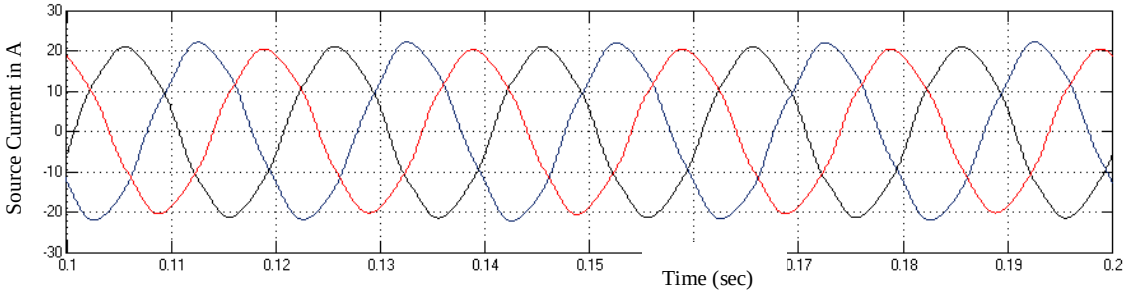

Figure 13(b): Source Current Waveform For Modified SRF Theory

The THD analyses for load and source currents are shown in Fig. 13(c) and 13(d)

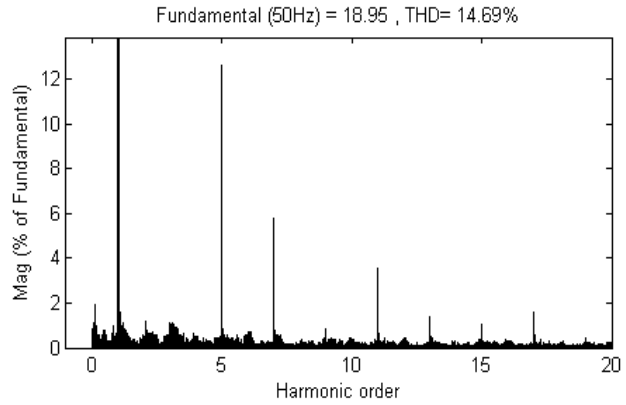

Figure 13(c): Load current THD

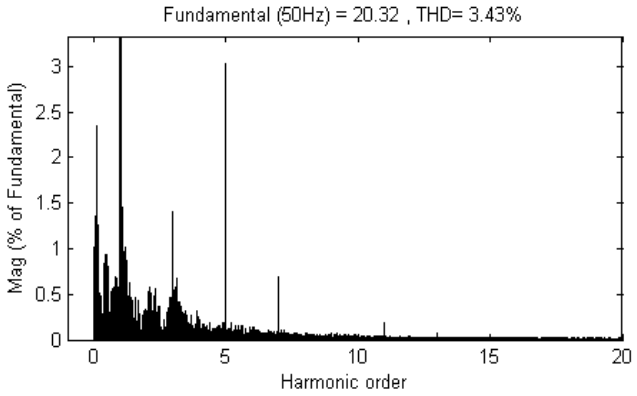

Figure 13(d): Source current THD

The DC bus voltage waveform is depicted in Fig.14.

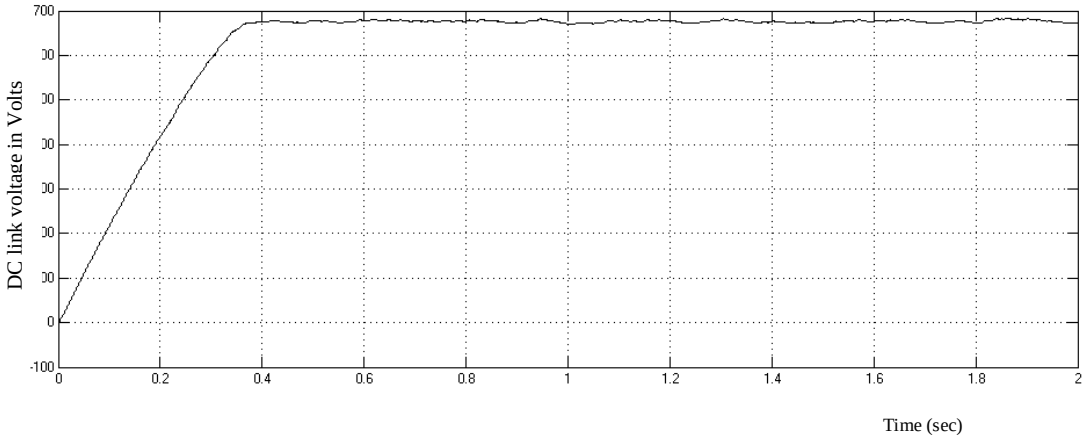

Figure 14: DC bus voltage

The above waveforms show the load and source current for all the three control strategies with the THD analysis. Tabulation below shows the comparison of the control techniques.

Table 2: Comparison of The Performance of Different Control Strategies

Control Strategy	Load Current THD %	Source Current THD%
SRF theory	15.71	3.07
Adaptive Filter	16.22	3.42
Modified SRF theory	14.69	3.43

From Table 2, it is inferred that SRF control strategy performs better in the mitigation of harmonics in the source current. Using SRF Theory the %THD is reduced from 15.71% to 3.07% whereas Adaptive filter decreases 16.22% to 3.42% and Modified SRF theory reduces 14.69% to 3.43%. When the execution speed is compared, Adaptive filter is quickest among all the control strategies. In Adaptive filter, the speed can be varied using the internal constants which are used in the controller.

Conclusion

DSTATCOM with Solar panel and boost converter are implemented for a 3-phase distribution system with different control strategies. The %THD of source current is well below 5% according to IEEE-519 standards. The DC link voltage is maintained constant in all the three control strategies using the solar panel and a boost converter. The comparison is performed under varying load and source conditions. These results are obtained for non-linear and unbalanced load conditions.

Appendix -1

3-phase line voltage : 415V, 50Hz
Line impedance : 8Ω and 19mH
Non-linear Load : 3-phase diode bridge rectifier with 27Ω and 10mH
Unbalanced load : 27Ω + 20mH (R-phase), 10Ω + 20mH (Y-phase), 27Ω + 10mH (B-phase)
Ripple filter : 1Ω and 100μF
AC inductor : 25mH
DC link capacitor : 3000μF
DC link voltage : 678V

References

[1] V. Kamatchi Kannan and N. Rengarajan, 2012,"Photovoltaic based distribution static compensator for power quality improvement," *International Journal of Electrical Power and Energy Systems*, 42(1), pp. 685-692.

[2] Pinto JP, Pregitzer R, Monteiro LFC and Afonso JL, 2007, " 3-Phase 4-wire shunt active filter with renewable energy interface*," IEEE Conference on renewable energy & power quality*.

[3] Jan T and Bialasiewicz, 2008,"Renewable energy systems with photovoltaic power generators: operation and modelling*," IEEE Trans Ind Electron*, 55(7), pp.2752-2758.

[4] Lo Y, Lee T and Wu K, 2008," Grid-connected photovoltaic system with power factor correction," *IEEE Trans Ind Electron*, 55(5), pp. 2224–2227.

[5] Dursun Erkan and Kilic Osman, 2012," Comparative evaluation of different power management strategies of a stand-alone PV/Wind/PEMFC hybrid power system," *International Journal of Electrical Power and Energy Systems*, 34(1), pp.81-89.

[6] Changchien SK, Liang TJ, Chen JF and Yang S, 2010," Novel high step-up DC–DC converter for fuel cell energy conversion system," *IEEE Trans Ind Electron*, 57(6), pp.2007-2017.

[7] J. Jacobs, D. Detjen, C. U. Karipidis, and R. W. De Doncker, 2004, "Rapid prototyping tools for power electronic systems: Demonstration with shunt active power filters," *IEEE Trans. Power Electron.*, 19(2), pp. 500–507.

[8] Bhim Singh, Sabha Raj Arya, Ambrish Chandra and Kamal Al-Haddad, 2014," Implementation of Adaptive Filter in Distribution Static Compensator*," IEEE Trans. on Ind App*, 50(5), pp.3026-3036, Oct. 2014

[9] K. R. Padiyar, 2008, *FACTS Controllers in Power Transmission and Distribution*. New Delhi, India: New Age Int.

[10] S. B. Karanki, N. Geddada, M. K. Mishra, and B. K. Kumar, 2012, "A DSTATCOM topology with reduced DC-link voltage rating for load compensation with non-stiff source," *IEEE Trans. Power Electron.*, 27(3), pp. 1201–1211.

[11] P. Karuppanan and Kamala Kanta Mahapatra, 2014, "Active harmonic current compensation to enhance power quality," *International Journal of Electrical Power and Energy Systems*, 62(1), pp.144-151.

[12] Merabet L, Saad S, Ould Abdeslam D and Omeiri.A, 2013," A comparative study of harmonic currents extraction by simulation and implementation," *International Journal of Electrical Power and Energy Systems*, 53(1), pp.507–514.